

Epithelial ovarian cancer stem-like cells are resistant to the cellular lysis of cytokine-induced killer cells via HIF1A-mediated downregulation of ICAM-1

SHIXIA BU¹, BONING LI¹, QIAN WANG¹, TINGTING GU¹, QIANGGANG DONG²,
XIAOFEI MIAO² and DONGMEI LAI¹

¹The International Peace Maternity and Child Health Hospital, School of Medicine, Shanghai Jiaotong University, Shanghai 200030; ²Shanghai iCELL Biotechnology Co., Ltd., Shanghai 200333, P.R. China

Received February 26, 2018; Accepted February 22, 2019

DOI: 10.3892/ijo.2019.4794

Abstract. Epithelial ovarian cancer (EOC) is the most lethal of all gynecologic tumors. Cancer spheroid culture is a widely used model to study cancer stem cells. Previous studies have demonstrated the effectiveness of cytokine-induced killer (CIK) cell-based therapies against cancer and cancer stem cells. However, it is not clear how EOC spheroid cells respond to CIK-mediated cellular lysis, and the mechanisms involved have never been reported before. A flow cytometry-based method was used to evaluate the anti-cancer effects of CIK cells against adherent A2780 cells and A2780 spheroids. To demonstrate the association between hypoxia inducible factor-1 α (HIF1A) and intercellular adhesion molecule-1 (ICAM-1), two HIF1A short hairpin RNA (shRNA) stable transfected cell lines were established. Furthermore, the protein expression levels of hypoxia/HIF1A-associated signaling pathways were evaluated, including transforming growth factor- β 1 (TGF- β 1)/mothers against decapentaplegic homologs (SMADs) and nuclear factor- κ B (NF- κ B) signaling pathways, comparing A2780

adherent cells and cancer spheroids. Flow cytometry revealed that A2780 spheroid cells were more resistant to CIK-mediated cellular lysis, which was partially reversed by an anti-ICAM-1 antibody. HIF1A was significantly upregulated in A2780 spheroids compared with adherent cells. Using HIF1A shRNA stable transfected cell lines and cobalt chloride, it was revealed that hypoxia/HIF1A contributed to downregulation of ICAM-1 in A2780 spheroid cells and adherent cells. Furthermore, hypoxia/HIF1A-associated signaling pathways, TGF- β 1/SMADs and NF- κ B, were activated in A2780 spheroid cells by using western blotting. The findings indicate that EOC stem-like cells resist the CIK-mediated cellular lysis via HIF1A-mediated downregulation of ICAM-1, which may be instructive for optimizing and enhancing CIK-based therapies.

Introduction

Epithelial ovarian cancer (EOC) remains the most lethal gynecological cancer threatening women worldwide, due to its late presentation, metastasis, recurrence and chemo-resistance. Although various forms of therapy have been created, >70% of patients relapse within 18 months (1). Ovarian cancer stem cells are a specific population of tumor cells with tumor initiation and self-renewal ability (2), which are potentially responsible for chemo-resistance, invasion/metastasis, tumor immune privilege and poor prognosis (3).

Cancer multicellular spheroids cultured in suspension system or three-dimensional culture are widely used approaches to investigate cancer stem cells. Numerous researchers have demonstrated that culturing cancer cells in suspension to form spheroids is a more accurate reflection and imitation of clinical cancer behavior *in vitro* than traditional adherent culture system (4-7). Cancer spheroids exhibit resistance to apoptosis-inducing drugs (4), and have notably different metabolic profiles (5) and signaling pathways compared with individual cancer cells (6). 3D culture systems have gained increasing attention and recognition as tools for researching antitumor drugs, molecular regulation mechanisms in cancer stem cells and establishment of personalized cancer therapy (7).

The standard front-line therapy for EOC is a combination of debulking surgery and platinum-based chemotherapy.

Correspondence to: Professor Dongmei Lai, The International Peace Maternity and Child Health Hospital, School of Medicine, Shanghai Jiaotong University, 910 Hengshan Road, Xuhui, Shanghai 200030, P.R. China
E-mail: laidongmei@hotmail.com

Abbreviations: EOC, epithelial ovarian cancer; CIK, cytokine-induced killer; HIF1A, hypoxia inducible factor-1 α ; ICAM, intercellular adhesion molecule; CoCl₂, cobalt chloride; rhTGF- β 1, recombinant human transforming growth factor- β 1; SMADs, mothers against decapentaplegic homologs; NK, natural killer; PBMC, peripheral blood mononuclear cells; PBS, phosphate-buffered saline; FBS, fetal bovine serum; E:T, effector cells to target cells ratio; PCR, polymerase chain reaction; CFSE, 5- or 6-(N-succinimidyl)oxycarbonyl fluorescein 3',6'-diacetate

Key words: epithelial ovarian cancer, cancer stem-like cell, cytokine-induced killer cells, hypoxia inducible factor-1 α , intercellular adhesion molecule-1

Certain preclinical and clinical studies have reported the benefits of adoptive immunotherapy in EOC, including human leukocyte antigen-restricted tumor infiltrating lymphocytes (8) and MHC-independent immune effectors such as natural killer (NK) cells (9), lymphokine-activated killer (10) and cytokine-induced killer (CIK) cells (11,12).

CIK cells are a heterogeneous population of CD3⁺CD56⁺NK T cells that were first discovered in the 1990s (13). CIK cells are generated from human peripheral blood mononuclear cell (PBMCs) and can be easily expanded *in vitro*. Numerous basic research investigations and clinical studies have demonstrated the safety and efficiency of CIK-based therapies in treating malignant tumors *in vitro* and *in vivo*, including the role of CIK in killing cancer stem cells (14).

In this study, it was aimed to identify the effects of CIK cells on ovarian cancer spheroid cells to determine the mechanism involved in resistance to CIK cells.

Materials and methods

Collection of PBMCs. This study was approved by the Institutional Ethics Committee of the International Peace Maternity and Child Health Hospital and Shanghai Red Cross Blood Center (Shanghai, China). Written informed consent was obtained from all participants. Criteria for donors were no history of chronic diseases (including diabetes and hypertension), viral infections (such as hepatitis), autoimmune diseases (including systemic lupus erythematosus, rheumatoid arthritis and nephritis) and cancer.

Isolation of PBMC, culture and characterization of CIK cells. Blood samples (n=20) were collected at the Shanghai Blood Center between January 2016 and December 2016. The male to female ratio of donors was 1:1. Age range of donors was 28–42 years old. Peripheral blood (20 ml) was collected with EDTA anticoagulant from each donor and centrifuged at 400 x g for 10 min to remove plasma at 4°C. The blood cell pellet was resuspended in 20 ml phosphate-buffered saline (PBS) and centrifuged at 800 x g for 15 min in Ficoll centrifuge tube at 4°C. PBMCs at the interface were collected and resuspended in 40 ml PBS and centrifuged at 400 x g for 10 min at 4°C. The cell pellet was resuspended in 40 ml PBS and centrifuged at 400 x g for 10 min at 4°C for the second time. PBMCs were adjusted to 1x10⁶ cells/ml and cultured in 10 ml GT-T551 culture medium (Takara Bio, Inc., Otsu, Japan) supplemented with 10% fetal bovine serum (FBS; Thermo Fisher Scientific, Inc., Waltham, MA, USA), 1,000 U/ml interferon- γ (Shanghai Chemo Wanbang Biopharma Co., Ltd., Shanghai, China) in T25 flask for 24 h at 37°C with 5% CO₂. Then cells were stimulated with 30 ng/ml anti-CD3 antibody (cat. no. TL-101, T&L Biological Technology, Beijing, China) and 1,000 IU/ml interleukin-2 (IL-2; Shanghai Huaxin High Biotechnology, Inc., Shanghai, China) to induce CIK cell proliferation. The cell culture was supplemented with 1,000 IU/ml IL-2 every 2 days.

To characterize CIK cells induced from PBMCs, cells were harvested and suspended in ice cold PBS with 10% FBS. Then cells were stained with labeled primary antibodies according to the technical data sheet as follows: CD3-fluorescein isothiocyanate (cat. no. 300305; 1:20; BioLegend, Inc., San Diego, CA, USA), and CD56-allophycocyanin (cat. no. 362503; 1:20;

BioLegend, Inc.) for 30 min at 4°C. Then cells were washed in cold PBS and analyzed using a flow cytometer (Accuri C6; BD Biosciences, Franklin, Lakes, NJ, USA).

Cancer cell lines. A2780 epithelial ovarian cancer cell line was obtained from the Shanghai Cell Bank of Chinese Academy of Sciences (Shanghai, China) and cultured in Dulbecco's modified Eagle's medium (DMEM)/high glucose (Thermo Fisher Scientific, Inc.) medium supplemented with 10% FBS, streptomycin (100 U/ml) and penicillin (100 U/ml). Cancer spheroid cells were cultured in DMEM/F12 (Thermo Fisher Scientific, Inc.) medium supplemented with 10% knock-out serum (Thermo Fisher Scientific, Inc.), streptomycin (100 U/ml; Thermo Fisher Scientific, Inc.), penicillin (100 U/ml; Thermo Fisher Scientific), 1X non-essential amino acids (Thermo Fisher Scientific, Inc.), 1 mM sodium pyruvate (Thermo Fisher Scientific, Inc.), 20 ng/ml human recombinant epidermal growth factor, and 10 ng/ml basic fibroblast growth factor. Cobalt chloride (CoCl₂; Sigma-Aldrich; Merck KGaA, Darmstadt, Germany) was used to induce chemical hypoxia. Recombinant human transforming growth factor- β 1 protein (rhTGF- β 1; Abcam, Cambridge, UK) was used to treat cancer cells for 24 h and then used for subsequent experiments. All cells were incubated at 37°C in an incubator containing 5% CO₂.

Immunofluorescence (IF) staining. Aldehyde dehydrogenase 1 family member A1 (ALDH1A1) and Nanog were identified by using the indirect immunofluorescent labeling technique. Cells (80% confluence) were fixed with 4% paraformaldehyde for 15 min at room temperature. After washing in PBS with 0.1% Tween-20 three times, samples were permeabilized using PBS containing 0.25% Triton X-100 for 10 min at room temperature. After washing in PBS with 0.1% Tween-20 three times, samples were blocked by PBS containing 1% bovine serum albumin (Yeasen, Shanghai, China), 22.52 mg/ml glycine and 0.1% Tween-20 for 30 min at room temperature, and then incubated with the following primary antibodies at 4°C overnight: ALDH1A1 (cat. no. ab52492; 1:200; Abcam) and Nanog (cat. no. ab109250; 1:200; Abcam). Subsequently, cells were incubated with secondary antibody conjugated to Alexa Fluor[®] 488 (cat. no. A-11008; 1:200; Thermo Fisher Scientific, Inc.). Cells were counterstained with DAPI (Thermo Fisher Scientific, Inc.) and examined under the fluorescence microscope (three fields of each sample were evaluated; Leica Microsystems GmbH, Wetzlar, Germany).

Flow cytometry-based cytotoxic activity assay. Target cells (adherent cancer cells and cancer spheroid cells of 80% confluence) in 2 ml PBS were labeled with 5 μ M fluorescent dye 5- or 6-(N-succinimidyl)oxycarbonyl fluorescein 3',6'-diacetate (CFSE; Beyotime Institute of Biotechnology, Haimen, China) at 37°C for 10 min and terminated by addition of 1 ml FBS. The fluorescence-labeled cells were washed in PBS three times, resuspended in complete culture medium, and adjusted cell density to 1x10⁶ cells/ml. CIK cells were collected, resuspended in complete culture medium and adjusted cell density to 1x10⁷ cells/ml. To evaluate cellular lysis effects of CIK cells on cancer cells in different E:T and at different time, different number of CIK cells were mixed with 100,000 target cells (adherent cells and cancer spheroids) to set the ratio of

effector cells (CIK cells) to target cells (cancer cells) (E:T) at 5: 1, 10:1 or 20:1. The death rate of target cells untreated with CIK cells was considered as the ratio of the spontaneous cell death. The mixture of target cells and CIK cells were centrifuged at 400 x g for 5 min and cultured at 37°C for 4, 24 and 48 h. To evaluate the death of cancer cells, propidium iodide (PI; 100 mg/ml, 20 µl/test; Sigma-Aldrich; Merck KGaA) was used. Following addition of PI, cells were incubated at 4°C for 15 min, washed in PBS, resuspended in 100 µl PBS, and then analyzed by flow cytometry (Accuri C6; BD Biosciences). Specific cytotoxicity (%) was calculated according to the formula: Specific killing efficiency = (target cells from PI⁺/CFSE⁺ quadrant - spontaneous death)/(100 - spontaneous death) x 100 (12).

RNA extraction and reverse transcription-quantitative polymerase chain reaction (RT-qPCR). Total RNA was extracted from cultured cells using TRIzol (Thermo Fisher Scientific, Inc.). RT to produce cDNA was performed using PrimeScript[™] RT reagent kit with gDNA Eraser (Takara Bio, Inc.) according to the manufacturer's instructions. qPCR reactions were performed using the SYBR Green Real-time PCR Master Mix (Takara Bio, Inc.). PCR primers were designed according to cDNA sequences in the NCBI database. The following primers were used: 18s RNA, forward 5'-CGTTGATTAAGTCCCTGC CCTT-3' and reverse 5'-TCAAGT TCGACCGTCTTCTCAG-3'; intercellular adhesion molecule (ICAM)-1, forward 5'-GAACC TTACCCTACGCTGCC-3' and reverse 5'-CAGTGC GGAC GAGAAATTG-3'; ICAM-2, forward 5'-GGTACACGTGAG GCCAAAGA-3' and reverse 5'-TTTCCACTGAGCCTGTT CGT-3'; ICAM-3, forward 5'-CCCAA AATTGACCGAGC CAC-3' and reverse 5'-ACGTTGACGAAGAACGGGAT-3'; HIF1A, forward 5'-GCACAGGCCACATTCACGTA-3' and reverse 5'-GGCTGTGTGCGACTGAGGAAA-3'. Cycling conditions for the PCR machine were as follows: 95°C for 5 sec, 60°C for 30 sec and 72°C for 30 sec for 40 cycles. All reactions were performed in a 10 µl volume. Gene expression levels were evaluated using the $\Delta\Delta Cq$ method (15), standardized to levels of 18s RNA amplification.

Western blot analysis. For western blotting, cells were lysed using RIPA (Yeasen) and protein concentration was determined by BCA Protein Assay Kit (Thermo Fisher Scientific, Inc.). Lysates (10-20 µg) were separated on by 10% SDS-PAGE gel and transferred to a polyvinylidene difluoride membrane (EMD Millipore, Billerica, MA, USA). Membranes were blocked with 5% non-fat milk in Tris-HCl buffer solution containing 0.1% Tween-20 (TBST) and were separately incubated in the following primary antibodies at 4°C overnight: ALDH1A1 (cat. no. ab52492, 1:1,000; Cell Signaling Technology, Inc., Danvers, MA, USA), Nanog (cat. no. ab109250, 1:1,000; Cell Signaling Technology, Inc.), β -actin (cat. no. 66009-1-Ig, 1:20,000; ProteinTech Group, Inc., Chicago, IL, USA), ICAM-1 (cat. no. ab53013, 1:1,000; Abcam), GAPDH (cat. no. 30203ES10, 1:5,000; Yeasen), HIF1A (cat. no. WL01607, 1:500; Wanleibio Co., Ltd., Shanghai, China), phosphor-mothers against decapentaplegic homolog 3 (phosphor-SMAD3; cat. no. ab52903, 1:1,000; Abcam), SMAD3 (cat. no. 9523, 1:1000; Cell Signaling Technology, Inc.), phosphor-SMAD2 (cat. no. ab188334,

1:1,000; Abcam), SMAD2 (cat. no. 5339, 1:1,000; Cell Signaling Technology, Inc.), TGF- β 1 (cat. no. ab64715, 1:1,000; Abcam), phospho-I κ B kinase (I κ B)- α/β (cat. no. 2697, 1:1000; Cell Signaling Technology, Inc.), phosphor-NF- κ B inhibitor (phosphor-I κ B; cat. no. 2859, 1:1,000; Cell Signaling Technology, Inc.), I κ B (cat. no. 4812, 1:1,000; Cell Signaling Technology, Inc.), phosphor-p65 (cat. no. 3031, 1:1,000; Cell Signaling Technology, Inc.), p65 (cat. no. 8242, 1:1,000; Cell Signaling Technology, Inc.), and vascular endothelial growth factor A (VEGFA; cat. no. ab52917, 1:1000; Abcam). Following washing with TBST, membranes were incubated with horseradish peroxidase-conjugated anti-rabbit IgG (cat. no. 33101ES60, 1:2,500; Yeasen). Visualization of blots was performed using a standard protocol for electro-chemiluminescence (cat. no. P10100, New Cell & Molecular Biotech Co., Suzhou, China). Levels of GAPDH or β -actin were used as internal standards.

Flow cytometry-based method for evaluating cell cycle distribution and anoikis. To assess the cell cycle progression of adherent cells and cancer spheroids of A2780 (80% confluence), cells were harvested and fixed with 70% ethanol at -20°C. After 24 h, cells were stained with 0.1 mg/ml PI (Sigma-Aldrich; Merck KGaA) and cell cycle distribution was evaluated by flow cytometry (Accuri C6; BD Biosciences).

To assess the anoikis-resistance of adherent cells and cancer spheroids of A2780 (80% confluence), cells were harvested and cultured in sterile flow cytometry tube at 37°C. After 24 or 48 h, cells were stained with 0.1 mg/ml PI and the positive rates of PI were evaluated by flow cytometry (Accuri C6; BD Biosciences).

Blocking CIK-mediated lysis by using antibody against ICAM-1 on cancer cells. To block the function of ICAM-1 of cancer cells, cells were incubated with 10 µg/µl ICAM-1 antibody (cat. no. ab53013; Abcam) or GFP antibody (as a negative control; cat. no. ab183734; Abcam) in MACS buffer at 4°C for 30 min. Then cells were used for subsequent experiments.

Cell Counting Kit-8 (CCK-8) assay. Cell viability was detected with CCK-8 (Yeasen) according to the manufacturer's protocol. Cancer cells (5,000 cells per well) were seeded in 96-well plate with complete culture medium for 24 h. Then different number of CIK cells were added at different E:T ratios as follows: 25,000 CIK for 5:1, 50,000 CIK cells for 10:1 and 100,000 CIK cells for 20:1. After 24 h, cell viability was measured using Synergy microplate reader (BioTek Instruments, Inc., Winooski, VT, USA).

Construction of HIF1A knockdown plasmid and stable transfection. The pGPU6/short hairpin RNA (shRNA) construction for HIF1A and negative control (NC) were designed and purchased from Shanghai GenePharma Co., Ltd. (Shanghai, China). The shRNA sequences are as follows: HIF1A-KD-1, sense CACCGGGATTAAGTCACTTGAAGTTCAAGAG AAGTTCAAAGTGAAGTTAATCCCTTTTGTG, anti-sense GATCCAAAAAAGGGATTAAGTCACTTGAAGTTCTC TTGAAAGTTCAAAGTGAAGTTAATCCC; HIF1A-KD-2, sense CACCGGAAATGAGAGAAATGCTTACTTCAAG AGAGTAAGCATTCTCTCATTTCCTTTTGTG, anti-sense

GATCCAAAAAAGGAAATGAGAGAAATGCTTACTCTA TTGAAGTAAGCATTCTCTCATTTC; NC, sense CACC GTTCTCCGAACGTGTCACGTTTCAAGAGAACGTGAC ACGTTCGGAGAATTTTTTGG, anti-sense GATCCAAAAA ATTCTCCGAACGTGTCACGTTCTTGAACGTGACA CGTTCGGAGAAC. To establish shRNA cell lines, 1×10^5 A2780 cells were transfected with $1 \mu\text{g}$ pGPU6/shRNA constructs by Lipofectamine® 3000 (Thermo Fisher Scientific, Inc.) for 24 h and selected in complete medium containing $100 \mu\text{g}/\text{ml}$ neomycin for 14 days. The colonies stably expressing shRNAs were expanded and used for subsequent experiments.

ELISA. An ELISA kit was used to test whether A2780 spheroid cells secrete TGF- β 1. A2780 cells (2×10^5) were cultured in suspension conditions. After 48 h, culture supernatant was collected and tested using the kit according to the instructions of the manufacturer (cat. no. DB100B; R&D Systems, Inc., Minneapolis, MN, USA).

Statistical analysis. Data are presented as the mean \pm standard error. Student's t-test, one-way analysis of variance (ANOVA) or two-way ANOVA were used to evaluate statistical differences via GraphPad Prism version 6 (GraphPad Software, Inc., La Jolla, CA, USA). Tukey's multiple comparisons test was used to compare specific groups following ANOVAs. $P < 0.05$ was considered to indicate a statistically significant difference.

Results

A2780 cancer spheroid cells exhibit cancer stem cell characteristics. In our previous research, cancer stem-like cells were isolated with drug selection in SK-OV-3 ovarian cancer cell lines (16) and could be enriched in ovarian cancer spheroids (17). Other studies revealed that certain cancer stem cell-associated markers were upregulated in ovarian cancer spheroids, including ALDH1A1 (18) and Nanog (19). In the current study, western blot analysis demonstrated that the protein expressions of ALDH1A1 and Nanog were strongly upregulated in A2780 spheroids compared with in adherent cells (Fig. 1A). Furthermore, IF was performed to examine the protein expression of ALDH1A and Nanog between A2780 adherent cells and spheroid cells. These two stemness-related markers (green) were highly expressed in A2780 spheroid cells than adherent cells, indicating cancer stem cell-like cells were enriched in spheroid cells (Fig. 1B). The cell cycle distribution of A2780 adherent cells and A2780 spheroids was also determined. The population of G0/G1 phases increased and the population of S/G2/M phases decreased in ovarian cancer spheroids compared with adherent cells (Fig. 1C). To further evaluate the difference of proliferative ability between adherent cells and cancer spheroids, a flow cytometry-based method to detect anoikis was conducted. Following culture in tubes for 24 or 48 h, adherent cells and cancer spheroids were stained with PI to label dead cells. The rate of PI-positive stained cells was lower for A2780 spheroids than A2780 adherent cells (Fig. 1D). This result indicated that A2780 cancer spheroid exhibited a greater ability of anoikis-resistance in the anchorage-independent stage than adherent cells. Taken together, these data indicated that ovarian epithelial cancer spheroid cells have properties of cancer stem cells.

A2780 ovarian cancer spheroid cells resist CIK-mediated cellular lysis. CIK cells were generated from PBMCs donated from healthy donors. The efficiency of inducing CD3⁺CD56⁺ CIK cells was identified by flow cytometry. The positive rates of CD3, CD56 and CD3/CD56 cells were 95.20 ± 3.96 , 46.40 ± 1.84 , and $44.50 \pm 5.94\%$ (Fig. 2A). To evaluate the cytotoxic effects of CIK cells against adherent cells and spheroid cells, a flow cytometry-based method was used. CIK cells induced cell death of A2780 adherent cells *in vitro* time-dependently and dose-dependently (Fig. 2B). After 24 h, although CIK cells could induce death of A2780 spheroid cells dose-dependently, the cytotoxicity was significantly lower compared with the adherent cells (Fig. 2C). The effects of CIK cells against A2780 spheroid cells or A2780 adherent cells were as follows: 2.8 ± 0.5 vs. $22.9 \pm 1.1\%$ at E:T 5:1; 4.2 ± 3.1 vs. $47.5 \pm 0.4\%$ at E:T 10:1; 9.3 ± 1.4 vs. $55.8 \pm 5.7\%$ at E:T 20:1 (Fig. 2B). All these results indicate that A2780 epithelial ovarian cancer spheroid cells exhibited the ability to resist the cytotoxic effects mediated by CIK cells.

ICAM-1 is downregulated in A2780 spheroid cells. ICAMs are reported to be important for CIK-mediated cellular lysis via a role in recognizing tumor target cells (20). To determine whether downregulation of ICAMs in EOC spheroid cells contributes to evasion from CIK-mediated cytotoxic effects, the transcriptional expression of ICAM-1, -2 and -3 between A2780 adherent cells and spheroid cells was analyzed by RT-qPCR. The mRNA expression levels of ICAM-1, -2 and -3 were all downregulated in A2780 spheroid cells compared with in A2780 adherent cells (Fig. 3A). Additionally, the most significantly downregulated gene among ICAMs in A2780 spheroid cells was ICAM-1 (Fig. 3B). The mRNA expression levels of ICAM-2 and ICAM-3 were 3-fold and 15-fold higher than the expression level of ICAM-1 in A2780 spheroid cells, respectively. These results indicated the importance of ICAMs in resistance to CIK-mediated lysis of A2780 spheroid cells. To further evaluate the protein expression level of ICAM-1 between adherent and spheroid A2780 cells, western blot analysis was performed. ICAM-1 was significantly reduced in A2780 spheroid cells compared with adherent A2780 cells (Fig. 3C), which was consistent with the results of RT-qPCR (Fig. 3A). To further explore whether ICAM-1 was involved in CIK-induced cellular lysis against A2780 adherent cells, anti-ICAM-1 antibody was used to directly block the function of ICAM-1 in A2780 adherent cells. The CCK-8 cellular viability assay demonstrated that adding antibody against ICAM-1 inhibited CIK-mediated cellular lysis and increased the viability of A2780 adherent cells dose-dependently *in vitro* (Fig. 3D), indicating that cell-cell interaction is required to mediate the cytotoxic effect of CIK cells, and ICAM-1 may be involved in cancer cell target recognition and cellular lysis by CIK cells. Additionally, anti-ICAM-1 antibody increased the viability of A2780 cells.

Knockdown of HIF1A in A2780 cells promotes CIK-mediated cellular lysis. Hypoxia occurs during tumor development. Hypoxia can be easily established in a 3D culture system *in vitro*. HIF1A is upregulated and expression is maintained in the core of cancer spheroids. HIF1A is also one of the most important hypoxia-related transcription factors that control

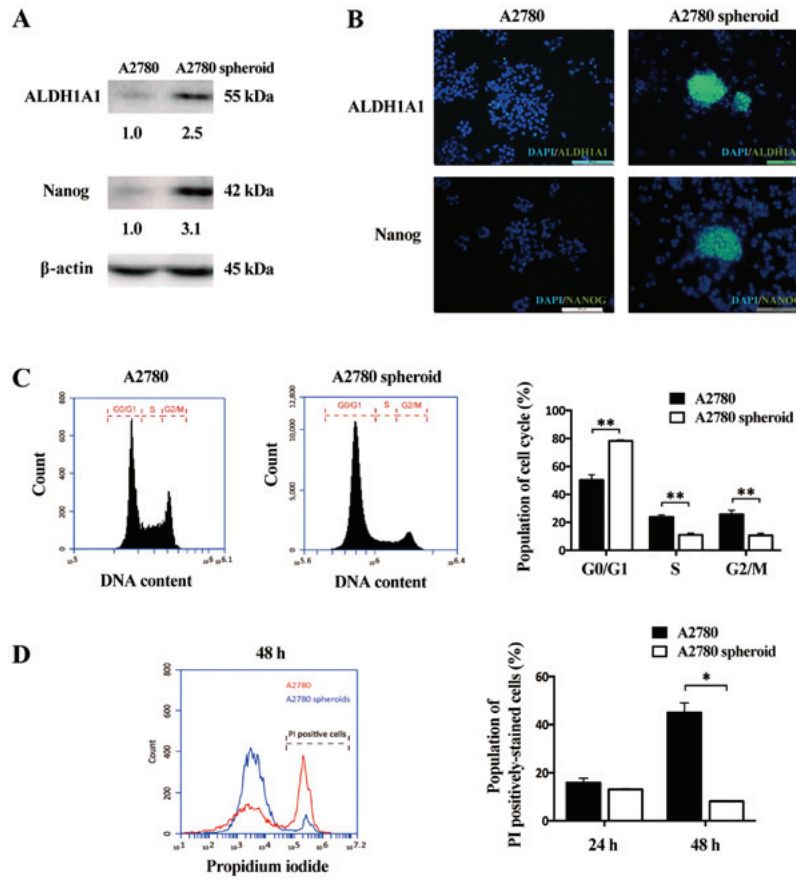


Figure 1. A2780 spheroid cells exhibited cancer stem-cell characteristics. (A) Western blotting for cancer stem cell-associated proteins, ALDH1A1 and Nanog in A2780 spheroid cells compared with A2780 adherent cells. (B) Immunofluorescence of ALDH1A and Nanog (green) in A2780 adherent cells and spheroid cells. DAPI (blue) staining of nuclei (scale bar, 100 μ m). (C) Flow cytometry-based cell cycle analysis of the population of G0/G1, S and G2/M phases in A2780 adherent cells and A2780 spheroid cells. (D) A flow cytometry-based method to detect anoikis between adherent cells and cancer spheroids. PI was used to stain dead cells. PI was used to stain dead cells and flow cytometry used to determine cell death in A2780 spheroid and A2780 adherent cells. Data are presented as the mean \pm standard error (n=3). *P<0.05 and **P<0.01. ALDH1A1, aldehyde dehydrogenase 1 family member A1; PI, propidium iodide.

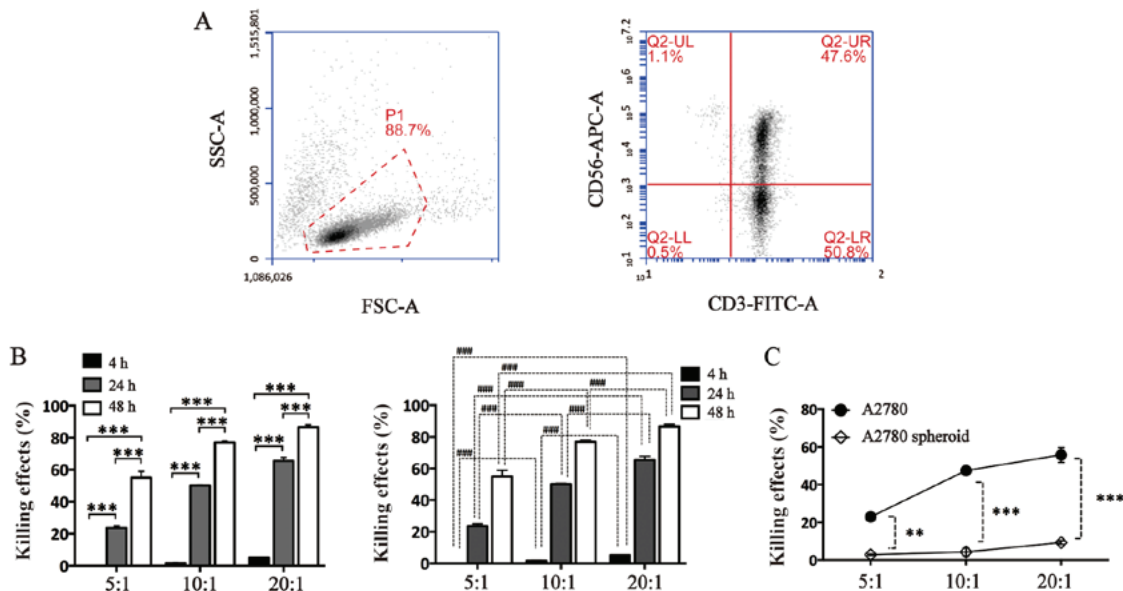


Figure 2. A2780 ovarian cancer spheroid cells are resistant to CIK-mediated cellular lysis. (A) Efficiency of inducing CIK cells evaluated by analyzing the positive rate of CD3 and CD56 of CIK cells using flow cytometry. The positive rate of CD3/CD56 was 44.50 \pm 5.94%. (B) Cell death effects of CIK cells against A2780 adherent cells at different E:T ratios and times (4, 24 and 48 h). CFSE was used to label cancer cells and PI was used to stain dead cells. Both CFSE-positive and PI-positive cells presented dead A2780 cells. (C) A2780 adherent cells and spheroid cells treated with CIK cells at different E:Ts for 24 h. Data are presented as the mean \pm standard error (n=3). *P<0.01 and *** or ###P<0.001. Two-way analysis of variance was used in B. CIK, cytokine-induced killer cells; E:T, effector cells to target cells; SSC, side scatter; FSC, forward scatter; APC, allophycocyanin; FITC, isothiocyanate; CFSE, 5- and 6-(N-succinimidylloxycarbonyl) fluorescein 3',6'-diacetate; PI, propidium iodide.

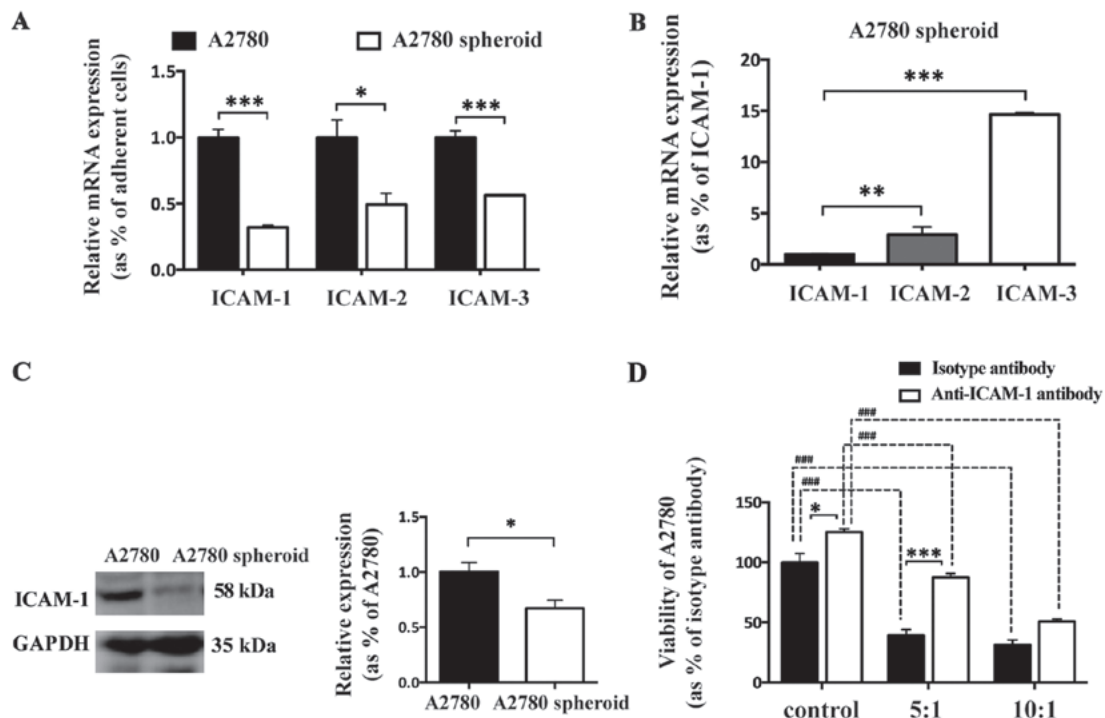


Figure 3. ICAM-1 is downregulated in A2780 cancer spheroid cells. (A) Reverse transcription quantitative polymerase chain reaction analysis of the mRNA expression levels of ICAM-1, -2 and -3 in A2780 spheroid cells compared with adherent cells. (B) The mRNA expression level of ICAM-1 in A2780 spheroid cells compared with the mRNA expression levels of ICAM-2 and ICAM-3. (C) Western blot analysis of ICAM-1 in A2780 spheroid cells compared with adherent cells. (D) Using Cell Counting Kit-8 cell viability analysis of CIK-mediated cellular lysis at different effector cells to target cells ratios and blocking of ICAM-1 in A2780 adherent cells with anti-ICAM-1 antibody cells. Data are presented as the mean \pm standard error (n=3). * P <0.05, ** P <0.01 and *** or ### P <0.001. One-way ANOVA was used in B. Two-way ANOVA was used in D. CIK, cytokine-induced killer cells; ANOVA, analysis of variance; ICAM, intercellular adhesion molecule.

the production of pro-angiogenic molecules and cancer stem cell-like traits in EOC cells (21). Western blot analysis demonstrated that HIF1A was significantly upregulated in A2780 spheroid cells compared with adherent cells (Fig. 4A). To explore whether HIF1A contributes to the resistance to CIK-mediated cellular lysis of spheroid cells, HIF1A knockdown (A2780-HIF1A-KD-1 and -2) and negative control (A2780-NC) A2780 cell lines were established. RT-qPCR and western blot analysis demonstrated that expression of HIF1A was significantly downregulated at the mRNA and protein levels in the knockdown cells compared with the negative control group (Fig. 4B). A CCK-8 cell viability assay revealed that knockdown of HIF1A promoted the cytotoxic effects of CIK cells and decreased the viability of both adherent cancer cells and cancer spheroids at different E:Ts (Fig. 4C). Additionally, knockdown of HIF1A in A2780 cells slightly decreased cellular proliferation *in vitro* (Fig. 4D and E).

HIF1A regulates expression of ICAM-1 in A2780 spheroid cells. Previous studies reported that hypoxia promoted ICAM-1 expression in endothelial cells via activation of HIF-independent nuclear factor- κ B (NF- κ B) pathway (22) and C-C motif chemokine ligand 15/Janus kinase 2/signal transducer and activator of transcription 3 pathway (23). However, whether HIF1A regulates ICAM-1 expression in EOC spheroid cells has not been reported before. In the current study, the association between HIF1A and ICAM-1 in A2780 spheroid cells was evaluated. RT-qPCR demonstrated that the mRNA expression of ICAM-1

was lower in A2780-NC spheroid cells compared with A2780-NC adherent cells. However, in the comparison with A2780-HIF1A-KD adherent cells, the mRNA expression level of ICAM-1 was only slightly affected in the two HIF1A knockdown spheroid cells. In addition, the mRNA expression level of ICAM-1 in A2780-HIF1A-KD spheroid cells was higher than that in A2780-NC spheroid cells (Fig. 5A). Western blot analysis demonstrated that the protein expression level of ICAM-1 in A2780-NC spheroid cells was lower than that in A2780-NC adherent cells (Fig. 5B). Notably, knockdown of HIF1A did not have an effect on protein expression of ICAM-1 in adherent cells, but the protein expression of ICAM-1 significantly upregulated in HIF1A knockdown spheroid cells compared with NC spheroid cells (Fig. 5B). To further elucidate the association between hypoxia and ICAM-1 in EOC cells, CoCl_2 was used to induce chemical hypoxia and determine the effects of hypoxia/HIF1A *in vitro*. Controversial results have been reported regarding the effects of CoCl_2 -induced hypoxia on the expression of ICAM-1 in different cell lines *in vitro*. It was reported that CoCl_2 upregulated ICAM-1 expression in endothelial cells (24), but downregulated ICAM-1 in colorectal cancer cells (25). Western blot analysis demonstrated that CoCl_2 dose-dependently decreased the protein expression level of ICAM-1 in A2780 adherent cells (Fig. 5C). These observations indicated that HIF1A/hypoxia may regulate the expression of ICAM-1 in the formation of A2780 spheroids, and may be partially involved in the resistance of A2780 spheroid cells to CIK cells.

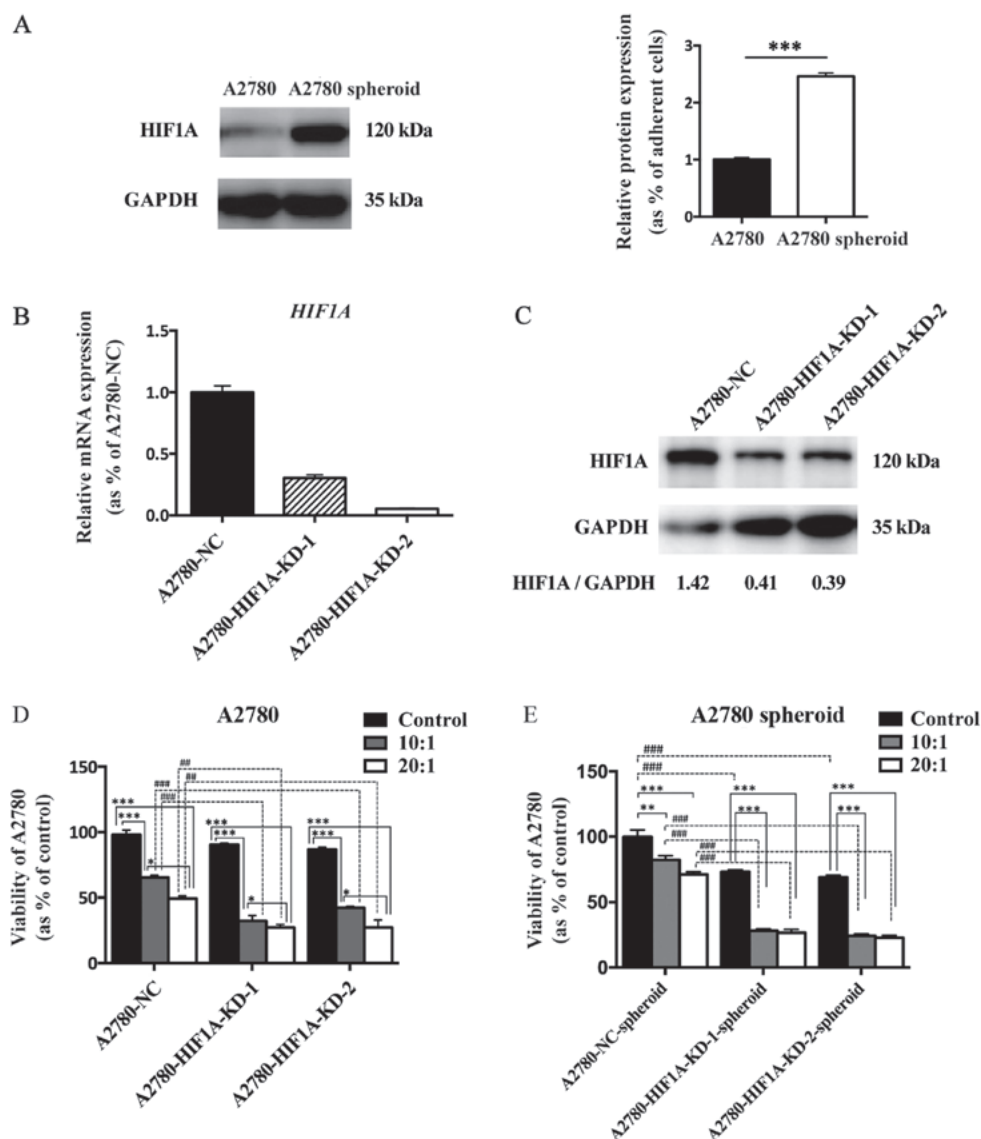


Figure 4. Knockdown of HIF1A in A2780 cells promotes CIK-mediated cellular lysis. (A) Western blot analysis of HIF1A in A2780 spheroid cells compared with A2780 adherent cells. (B) Two HIF1A knockdown plasmids were constructed and then two stable transfected A2780 cell lines (A2780-HIF1A-KD-1, -2) were established. Reverse transcription-quantitative polymerase chain reaction analysis of HIF1A at mRNA level. (C) Western blotting to determine the efficiency of HIF1A knockdown at protein level. (D) CCK-8 cell viability assay showed that knock-down of HIF1A in A2780 adherent cells and (E) cancer spheroids promoted CIK-mediated cellular lysis at E:T of 10:1 and 20:1 used. Data are presented as the mean \pm standard error (n=3). *P<0.05, ** or ##P<0.01 and *** or ###P<0.001. Two-way analysis of variance was used in E. CIK, cytokine-induced killer cells; CCK-8, Cell Counting Kit-8; E:T, effector cells to target cells; NC, negative control; HIF1A, hypoxia inducible factor-1 α ; KD, knockdown.

HIF1A-associated signaling pathways are activated in EOC cells. Various hypoxia-associated signaling pathways have been reported to be involved in the regulation of ICAM-1 expression, including TGF- β 1/SMADs and NF- κ B signaling pathway. The therapeutic potential of targeting TGF- β 1/SMADs (26) and NF- κ B signaling pathways (27) in ovarian cancer were also investigated. However, it is not clear whether TGF- β 1/SMADs and NF- κ B signaling pathways are active in EOC spheroids.

Western blot analysis demonstrated that the ratio of phosphor-SMAD3 to SMAD3 and phosphor-SMAD2 to SMAD2 were significantly increased in A2780 spheroid cells compared with in adherent cells. In addition, the protein expression level of TGF- β 1 was upregulated in A2780 spheroid cells compared with in A2780 adherent cells (Fig. 6A). To evaluate whether A2780 spheroid cells secrete TGF- β 1 into the

culture medium, an ELISA measuring TGF- β 1 was used. The amount of TGF- β 1 in the supernatant of A2780 spheroids was higher than that in fresh culture medium, which indicated that A2780 spheroids could secrete TGF- β 1 into culture medium (Fig. 6B). To further investigate the influence of TGF- β 1 on the transcriptional regulation of ICAM-1 in EOC cells, rhTGF- β 1 was added to treat A2780 adherent cells for 24 h. rhTGF- β 1 significantly decreased the mRNA expression level of ICAM-1 in A2780 cells (Fig. 6C).

Further results demonstrated that the phosphorylation level of Ikk- α/β , ratio of phosphor-I κ B to I κ B, and ratio of phosphor-p65 to p65 were all upregulated in A2780 spheroid cells compared with in adherent cells (Fig. 6D). In addition, the protein expression level of VEGFA was upregulated in A2780 spheroid cells compared with in adherent cells (Fig. 6E). These results indicated the increased activation of NF- κ B and

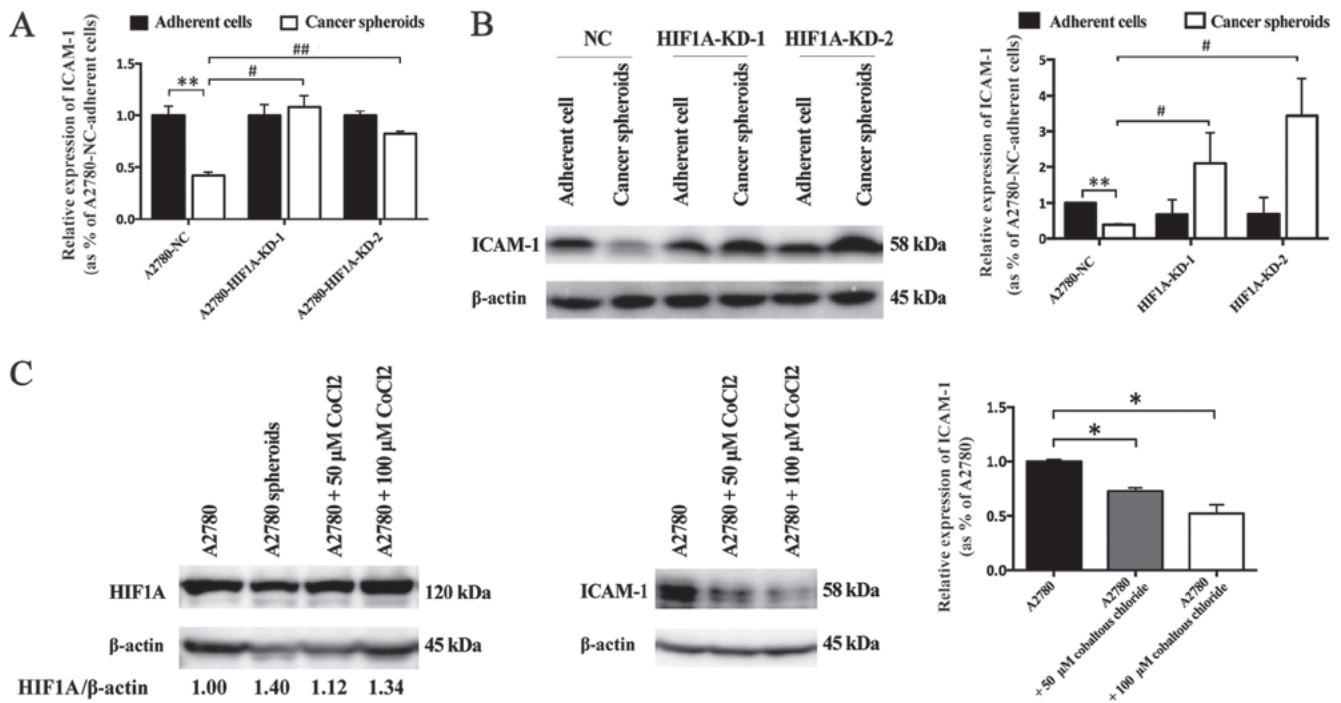


Figure 5. HIF1A regulates the expression of ICAM-1 in A2780 spheroid cells. (A) Reverse transcription-quantitative polymerase chain reaction analysis of ICAM-1 mRNA expression level in spheroid cells of A2780-negative control (A2780-NC) and A2780-NC adherent cells compared with A2780-HIF1A-KD spheroids. (B) Western blot analysis of the protein expression level of ICAM-1 in A2780-NC spheroid cells compared and A2780-NC adherent cells, and A2780-HIF1A-KD adherent cells and spheroid. (C) CoCl₂ was used to induce chemical hypoxia in A2780 cells followed by western blot analysis of the protein expression level of HIF1A and ICAM-1 in A2780 adherent cells. Data are presented as the mean \pm standard error (n=3). **P<0.05 and ***P<0.01. Data were analyzed by one-way analysis of variance. ICAM, intercellular adhesion molecule; NC, negative control; HIF1A, hypoxia inducible factor-1 α ; KD, knockdown.

TGF- β 1/SMADs signaling pathway in A2780 spheroid cells compared with adherent A2780 cells.

Discussion

Numerous studies have reported that epithelial cancer spheroid cells are more tumorigenic than their parental tumor cells, adherent cancer cells or differentiated cancer cells, including primary cells and EOC cell lines (7). The tumor-promoting trait is associated with the enrichment of ovarian cancer stem cells and activation of tumorigenic and stemness-associated signaling pathways in EOC spheroids (18). Condello *et al* (18) found that β -catenin-regulated ALDH1A1 was a target in ovarian cancer spheroids. Xu *et al* (19) observed that microRNA-214 regulates ovarian cancer cell stemness by targeting p53/Nanog. In this study, ALDH1A1 and Nanog were significantly upregulated in A2780 cancer spheroids, as determined via western blot analysis and immunofluorescence. A2780 spheroid cells exhibited higher capacity for self-renewal compared with adherent cells in a soft agar colony formation assay *in vitro*. Additionally, autophagy-mediated transition from G0 phase to G1 phase also contributes to the expression of OCT-4 and NOTCH1, two stemness-associated markers, in cancer spheroid cells (2). Determining the cell cycle distribution of A2780 and A2780 spheroid can provide the rate of G0/G1 phase, which is associated with cancer stem cells traits. Carduner *et al* (28) reported that ovarian cancer spheroid cells exhibited anoikis-resistance, which was important for survival of cancer cells; the present results are consistent with that. It is essential to confirm this trait as A2780 spheroid cells

exhibited anoikis-resistance. It may be concluded that the death of cancer cells is associated with CIK-mediated cellular lysis, but not anoikis. These results lead to the examination of stemness-associated markers (ALDH1A1 and Nanog) by western blot analysis and immunofluorescence, cell cycle distribution and anoikis-resistance via flow cytometry to investigate the differences, including in stemness, between adherent A2780 cancer cells and A2780 spheroids.

Cancer cells employ many mechanisms of immune escape, including downregulation of major histocompatibility complex (MHC) I expression (29), secretion of immune suppressive molecules (30), disrupting functions of immune cells and creating a tumor-favoring microenvironment (31). CIK cells have MHC-unrestricted activity against cancer stem cells, including in melanoma (32) and hepatocellular carcinoma (33). However, the effectiveness of CIK against EOC spheroids and whether spheroid cells endow the ability to evade immune attack has rarely been discussed previously.

ICAM-1 is well known for its anti-cancer function by recruiting immune cells (34). ICAM-1 is also important for recognition of tumor target cells of CIK cells. Some studies have reported the tumor-suppressive effects of ICAM-1 on ovarian cancer. Arnold *et al* (35) reported that ICAM-1 expressed at low levels in cancer cells and had a reverse association with patient survival. de Groote *et al* (36) showed an immune-independent cellular role of ICAM-1 in ovarian cancer, whereby upregulation of endogenous ICAM-1 reduced cancer cell growth in the absence of immune cells. Lymphocyte function-associated antigen 1/ICAM-1 are involved in target recognition leading to target cell lysis by CIK cells,

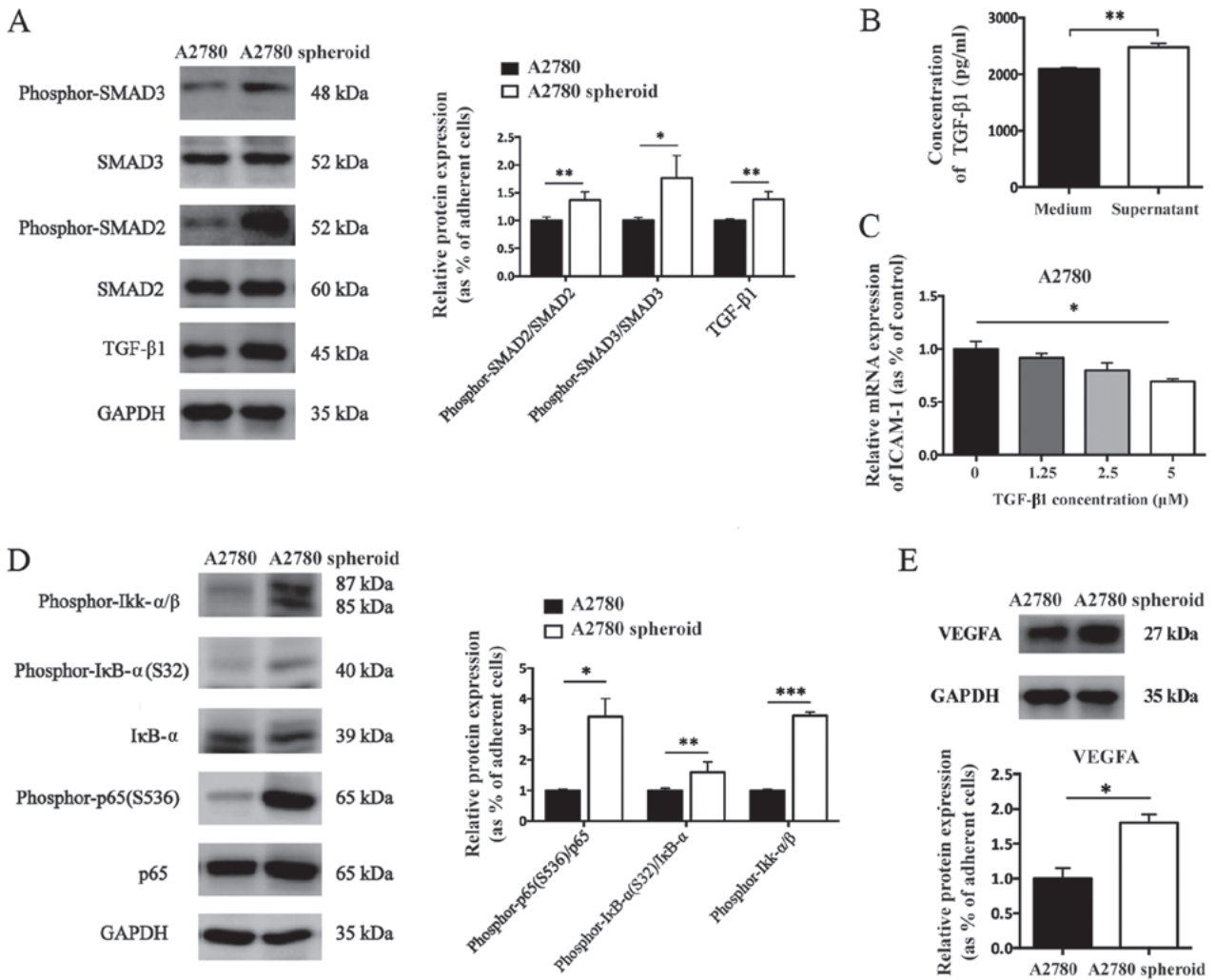


Figure 6. HIF1A-associated signaling pathways are activated in A2780 spheroid cells. (A) Western blot analysis of the phosphorylation level of SMAD2 and SMAD3 in A2780 spheroid cells compared with A2780 adherent cells and the protein expression level of TGF-β1 in A2780 spheroid cells compared with A2780 adherent cells. (B) ELISA analysis TGF-β1 concentration in A2780 spheroid cells culture medium and supernatant. (C) Recombinant human TGF-β1 was used to treat A2780 adherent cells for 24 h, and reverse transcription-quantitative polymerase chain reaction analysis of mRNA expression level of ICAM-1. (D) Western blot analysis was conducted to explore the activation level of nuclear factor-κB signaling pathway between A2780 adherent cells and spheroid cells. Phosphorylation of Ikk-α/β, IκBα and p65 in A2780 spheroid cells compared with adherent cells. (E) Western blot analysis displayed that protein expression level of VEGFA increased in A2780 spheroid cells compared to that in adherent cells. Data are presented as the mean ± standard error (n=3). *P<0.05, **P<0.01 and ***P<0.001. One-way analysis of variance was used in C. SMAD, mothers against decapentaplegic homolog 3; TGF-β1, transforming growth factor-β1; ICAM-1, intercellular adhesion molecule-1; Ikk-α/β, IκB kinase-α/β; IκBα, NF-κB inhibitor α; VEGFA, vascular endothelial growth factor A.

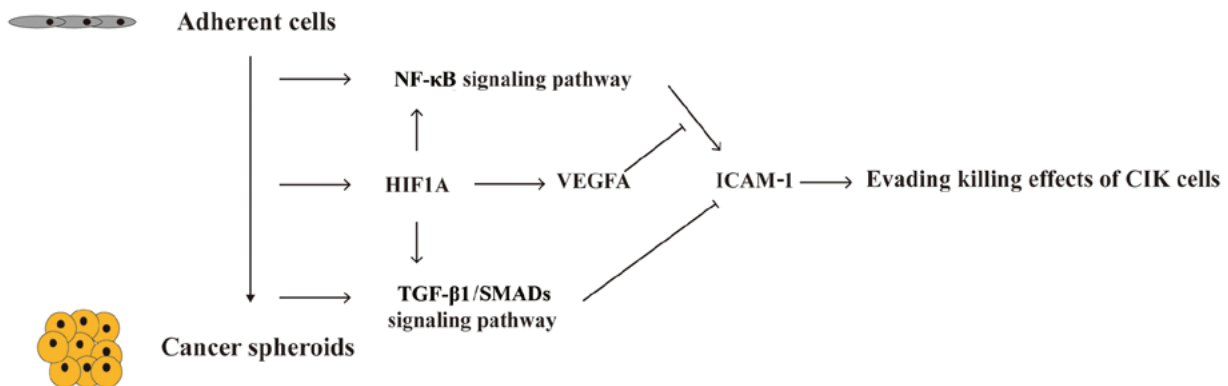


Figure 7. Schematic diagram showed that epithelial ovarian cancer spheroid cells endow the ability of evasion form CIK-mediated cellular lysis. Hypoxia/HIF1A-regulated downregulation of ICAM-1 is responsible for A2780 spheroid cells' resistance to immune attack of CIK cells. Furthermore, hypoxia/HIF1A-associated TGF-β1/SMADs and VEGFA signaling pathways might attribute to the downregulation of ICAM-1 in A2780 spheroid cells. NF-κB, nuclear factor-κB; HIF1A, hypoxia inducible factor-1α; VEGFA, vascular endothelial growth factor A; ICAM-1, intercellular adhesion molecule-1; CIK, cytokine-induced killer cells; TGF-β1, transforming growth factor-β1; SMAD, mothers against decapentaplegic homolog 3.

which can be blocked anti-ICAM-1 antibody. In the present study, the expression level of ICAM-1 was lower in ovarian cancer spheroids compared with in adherent cancer cells. Furthermore, blockage of ICAM-1 inhibited CIK-mediated cellular lysis in adherent cancer cells. These results suggest that ICAM-1 may have a role in the resistance to immune attack of ovarian cancer cells.

Tumor hypoxia and HIF1A are known to have important roles in ovarian cancer metastasis, angiogenesis and resistance to chemotherapy. In addition, the hypoxic tumor microenvironment and HIF1A contribute to immune escape in various cancer types, including prostate cancer, breast cancer (37). Terry *et al* (38) reported that HIF1A-dependent induction of epithelial-mesenchymal transition-associated transcription factors and secretion of immunosuppressive TGF- β enabled cancer cells to resist cytotoxic T cell and NK cell-mediated lysis. Furthermore, HIF1A-induced activation of PI3K/Akt, VEGFA/ERK, nitric oxide/cyclic GMP/protein kinase G signaling pathways promote immune evasion of cancer cells (39–41). MHC class I chain-related molecule A (MICA) is an NKG2D ligand that is also important for recognition of cancer cells and cancer stem cells by CIK cells in hepatocellular carcinoma (35), nasopharyngeal carcinoma (42). Barsoum *et al* (34) reported that hypoxia/HIF1A increased the expression of ADAM10 and decreased surface MICA levels on cancer cells, and contributed to resistance to lysis mediated by innate immune effectors, which was attenuated by using a nitric oxide mimetic. In the present study, EOC spheroid cells evaded CIK cells-mediated lysis, which was associated with HIF1A-mediated downregulation of ICAM-1. However, one cell line is not enough to avoid the significant variations among cancer cell lines due to their different genetic backgrounds. In future studies more suitable cell lines, animal models and clinical ovarian cancer samples will be used to further investigate the association among HIF1A, ICAM1 and immune reaction.

Various hypoxia-related signaling pathways are reported to be involved in the regulation of ICAM-1. Sawada *et al* (43) reported that TGF- β 1 decreased ICAM-1 expression in pancreatic cancer cells, inhibited lymphocyte-mediated cytotoxic effects and enhanced liver metastatic potential. Furthermore, Bessa *et al* (44) reported that immunoblockade of TGF- β 1 partially restored impaired leukocyte functions, indicating the immunosuppressive role of TGF- β 1. In the current study, A2780 spheroid cells could secrete TGF- β 1 and the TGF- β 1/SMADs signaling pathway was activated in A2780 spheroid cells. This observation indicates that TGF- β 1/SMADs signaling pathway may have important role in evasion from CIK cells in A2780 spheroid cells.

Additionally, NF- κ B signaling was activated in A2780 cancer spheroids, which is reported to facilitate upregulation of ICAM-1 in cardiovascular disorders (45). It was also observed that HIF1A-regulated VEGFA was upregulated in A2780 spheroid cells, which may have a role in inhibiting the expression of ICAM-1. Thichanpiang *et al* (46) reported that VEGF-A(165) b inhibited NF- κ B/tumor necrosis factor- α (TNF- α)-mediated upregulation of ICAM-1 expression in human retinal pigment epithelium cells. Li *et al* (47) also reported that NF- κ B promoted programmed cell death 1 ligand 1 (PD-L1) expression and fostered an immunosuppressive tumor microenvironment

in ovarian cancer, and the upregulation of PD-L1 promoted immune escape of cancer cells from CIK cells (48). Furthermore, combination of PD-L1/PD-1 blockade and CIK cells brought more benefits to patients with ovarian cancer (33). These results indicate that HIF1A-mediated upregulation of VEGFA may reduce the effects of NF- κ B/TNF- α on ICAM-1 in A2780 spheroid cells. Thus, the results of the present study suggest that hypoxia/HIF1A-induced downregulation of ICAM-1 is responsible for the resistance of A2780 spheroids to CIK-mediated cellular lysis. HIF1A-associated TGF- β 1/SMADs and VEGFA signaling pathways may mediate the downregulation of ICAM-1 in A2780 spheroid cells (Fig. 7).

CIK cell-based adoptive cell therapy (ACT) has exhibited activity in several pre-clinical models, suggesting that ACT may provide benefits in settings of low tumor burden, minimal residual disease or maintenance therapy. Liu *et al* (12) reported the clinical feasibility and efficacy of CIK cells in maintenance therapy against ovarian cancer, observing a significant increase in median progression free survival and no severe CIK cell infusion-associated toxicity. However, clinical research is still at early stage and few studies of CIK-based therapy in EOC have been conducted. Well-organized, individualized and combined cell therapy may promote its clinical effectiveness and application. Additionally, modifying CIK cells using chemical hetero-conjugation (11) and chimeric antigen receptors (49) may provide strategies to optimize and enhance CIK-based cancer therapy.

In conclusion, this work highlighted the HIF1A-mediated immune evasion of EOC spheroids from CIK cell-mediated lysis via downregulation of ICAM-1. Although CIK cells exhibit promising properties against many tumor and cancer stem cells, paying attention to the mechanisms of immune escape by cancer cells and identifying solutions to reduce evasion may generate more effective therapeutic strategies in ovarian cancer treatment.

Acknowledgements

The authors thank Chunhui Wang (Shanghai iCELL Biotechnology Co., Ltd.), Yan Zhang, Jing Gu and Jing Zhou for their technical advices. Thanks for Professor Hong Xu (Med-X Research Institute) and Dr Dingshengzi Zhang (Med-X Research Institute) for their assistance with flow cytometry.

Funding

This work was supported by grants from Shanghai Municipal Council for Science and Technology (grant no. 14411961500), Shanghai Municipal Education Commission-Gaofeng Clinical Medicine (grant no. 20152236), Shanghai Jiao Tong University Medicine-Engineering Fund (grant no. YG2015ZD11), The Interdisciplinary Program of Shanghai Jiao Tong University (grant no. YG2016MS43) and The National Natural Science Foundation of China under Grants (grant no. 81741013).

Availability of data and materials

The datasets used and/or analyzed during the current study are available from the corresponding author on reasonable request.

Authors' contributions

DL and SB participated in the design of the study. SB conducted the experiments. BL, QW, TG, QD and XM provided technical expertise and analyzed the data. SB prepared the manuscript and DL critically reviewed the manuscript. All authors have read and approved the final manuscript.

Ethics approval and consent to participate

This study was approved by the Institutional Ethics Committee of the International Peace Maternity and Child Health Hospital and Shanghai Red Cross Blood Center (Shanghai, China). Written informed consent was obtained from all participants.

Patient consent for publication

Not applicable.

Competing interests

The authors declare that they have no competing interests.

References

- Jayson GC, Kohn EC, Kitchener HC and Ledermann JA: Ovarian cancer. *Lancet* 384: 1376-1388, 2014.
- Wang Q, Bu S, Xin D, Li B, Wang L and Lai D: Autophagy is indispensable for the self-renewal and quiescence of ovarian cancer spheroid cells with stem cell-like properties. *Oxid Med Cell Longev* 2018: 7010472, 2018.
- You Y, Li Y, Li M, Lei M, Wu M, Qu Y, Yuan Y, Chen T and Jiang H: Ovarian cancer stem cells promote tumour immune privilege and invasion via CCL5 and regulatory T cells. *Clin Exp Immunol* 191: 60-73, 2018.
- Jeong JY, Kang H, Kim TH, Kim G, Heo JH, Kwon AY, Kim S, Jung SG and An HJ: MicroRNA-136 inhibits cancer stem cell activity and enhances the anti-tumor effect of paclitaxel against chemoresistant ovarian cancer cells by targeting Notch3. *Cancer Lett* 386: 168-178, 2017.
- Liao J, Qian F, Tchabo N, Mhawech-Fauceglia P, Beck A, Qian Z, Wang X, Huss WJ, Lele SB, Morrison CD, *et al*: Ovarian cancer spheroid cells with stem cell-like properties contribute to tumor generation, metastasis and chemotherapy resistance through hypoxia-resistant metabolism. *PLoS One* 9: e84941, 2014.
- Wang L, Mezencev R, Bowen NJ, Matyunina LV and McDonald JF: Isolation and characterization of stem-like cells from a human ovarian cancer cell line. *Mol Cell Biochem* 363: 257-268, 2012.
- Chen MW, Yang ST, Chien MH, Hua KT, Wu CJ, Hsiao SM, Lin H, Hsiao M, Su JL and Wei LH: The STAT3-miRNA-92-Wnt signaling pathway regulates spheroid formation and malignant progression in ovarian cancer. *Cancer Res* 77: 1955-1967, 2017.
- Chiriva-Internati M, Weidanz JA, Yu Y, Frezza EE, Jenkins MR, Kennedy RC, Cobos E and Kast WM: Sperm protein 17 is a suitable target for adoptive T-cell-based immunotherapy in human ovarian cancer. *J Immunother* 31: 693-703, 2008.
- Carlsten M, Björkström NK, Norell H, Bryceson Y, van Hall T, Baumann BC, Hanson M, Schedvins K, Kiessling R, Ljunggren HG, *et al*: DNAX accessory molecule-1 mediated recognition of freshly isolated ovarian carcinoma by resting natural killer cells. *Cancer Res* 67: 1317-1325, 2007.
- Law KS, Chen HC and Liao SK: Non-cytotoxic and sublethal paclitaxel treatment potentiates the sensitivity of cultured ovarian tumor SKOV-3 cells to lysis by lymphokine-activated killer cells. *Anticancer Res* 27: 841-850, 2007.
- Chan JK, Hamilton CA, Cheung MK, Karimi M, Baker J, Gall JM, Schulz S, Thorne SH, Teng NN, Contag CH, *et al*: Enhanced killing of primary ovarian cancer by retargeting autologous cytokine-induced killer cells with bispecific antibodies: A preclinical study. *Clin Cancer Res* 12: 1859-1867, 2006.
- Liu J, Li H, Cao S, Zhang X, Yu J, Qi J, An X, Yu W, Ren X and Hao X: Maintenance therapy with autologous cytokine-induced killer cells in patients with advanced epithelial ovarian cancer after first-line treatment. *J Immunother* 37: 115-122, 2014.
- Schmidt-Wolf IG, Negrin RS, Kiem HP, Blume KG and Weissman IL: Use of a SCID mouse/human lymphoma model to evaluate cytokine-induced killer cells with potent antitumor cell activity. *J Exp Med* 174: 139-149, 1991.
- Rong X, Wei F, Li A, Xiao D and Luo R: Effective activity of cytokine induced killer cells against hepatocellular carcinoma including tumor-initiating cells. *Med Hypotheses* 84: 159-161, 2015.
- Livak KJ and Schmittgen TD: Analysis of relative gene expression data using real-time quantitative PCR and the 2⁻(Delta Delta C(T)) Method. *Methods* 25: 402-408, 2001.
- Ma L, Lai D, Liu T, Cheng W and Guo L: Cancer stem-like cells can be isolated with drug selection in human ovarian cancer cell line SKOV3. *Acta Biochim Biophys Sin (Shanghai)* 42: 593-602, 2010.
- Luo X, Dong Z, Chen Y, Yang L and Lai D: Enrichment of ovarian cancer stem-like cells is associated with epithelial to mesenchymal transition through an miRNA-activated AKT pathway. *Cell Prolif* 46: 436-446, 2013.
- Condello S, Morgan CA, Nagdas S, Cao L, Turek J, Hurley TD and Matei D: β -catenin-regulated ALDH1A1 is a target in ovarian cancer spheroids. *Oncogene* 34: 2297-2308, 2015.
- Xu CX, Xu M, Tan L, Yang H, Permeth-Wey J, Kruk PA, Wenham RM, Nicosia SV, Lancaster JM, Sellers TA, *et al*: MicroRNA MiR-214 regulates ovarian cancer cell stemness by targeting p53/Nanog. *J Biol Chem* 291: 22851, 2016.
- Schmidt-Wolf IG, Lefterova P, Mehta BA, Fernandez LP, Huhn D, Blume KG, Weissman IL and Negrin RS: Phenotypic characterization and identification of effector cells involved in tumor cell recognition of cytokine-induced killer cells. *Exp Hematol* 21: 1673-1679, 1993.
- Qin J, Liu Y, Lu Y, Liu M, Li M, Li J and Wu L: Hypoxia-inducible factor 1 alpha promotes cancer stem cells-like properties in human ovarian cancer cells by upregulating SIRT1 expression. *Sci Rep* 7: 10592, 2017.
- Winning S, Splettstoesser F, Fandrey J and Frede S: Acute hypoxia induces HIF-independent monocyte adhesion to endothelial cells through increased intercellular adhesion molecule-1 expression: The role of hypoxic inhibition of prolyl hydroxylase activity for the induction of NF-kappa B. *J Immunol* 185: 1786-1793, 2010.
- Park KH, Lee TH, Kim CW and Kim J: Enhancement of CCL15 expression and monocyte adhesion to endothelial cells (ECs) after hypoxia/reoxygenation and induction of ICAM-1 expression by CCL15 via the JAK2/STAT3 pathway in ECs. *J Immunol* 190: 6550-6558, 2013.
- Goebeler M, Meinardus-Hager G, Roth J, Goerdts S and Sorg C: Nickel chloride and cobalt chloride, two common contact sensitizers, directly induce expression of intercellular adhesion molecule-1 (ICAM-1), vascular cell adhesion molecule-1 (VCAM-1), and endothelial leukocyte adhesion molecule (ELAM-1) by endothelial cells. *J Invest Dermatol* 100: 759-765, 1993.
- Kawczyk-Krupka A, Czuba ZP, Kwiatek B, Kwiatek S, Krupka M and Sieroń K: The effect of ALA-PDT under normoxia and cobalt chloride (CoCl₂)-induced hypoxia on adhesion molecules (ICAM-1, VCAM-1) secretion by colorectal cancer cells. *Photodiagn Photodyn Ther* 19: 103-115, 2017.
- Rynne-Vidal A, Au-Yeung CL, Jiménez-Heffernan JA, Pérez-Lozano ML, Cremades-Jimeno L, Bárcena C, Cristóbal-García I, Fernández-Chacón C, Yeung TL, Mok SC, *et al*: Mesothelial-to-mesenchymal transition as a possible therapeutic target in peritoneal metastasis of ovarian cancer. *J Pathol* 242: 140-151, 2017.
- Yan XY, Zhang Y, Zhang JJ, Zhang LC, Liu YN, Wu Y, Xue YN, Lu SY, Su J and Sun LK: p62/SQSTM1 as an oncotarget mediates cisplatin resistance through activating RIP1-NF- κ B pathway in human ovarian cancer cells. *Cancer Sci* 108: 1405-1413, 2017.
- Carduner L, Picot CR, Leroy-Dudal J, Blay L, Kellouche S and Carreiras F: Cell cycle arrest or survival signaling through α v integrins, activation of PKC and ERK1/2 lead to anoikis resistance of ovarian cancer spheroids. *Exp Cell Res* 320: 329-342, 2014.
- Aust S, Felix S, Auer K, Bachmayr-Heyda A, Kenner L, Dekan S, Meier SM, Gerner C, Grimm C and Pils D: Absence of PD-L1 on tumor cells is associated with reduced MHC I expression and PD-L1 expression increases in recurrent serous ovarian cancer. *Sci Rep* 7: 42929, 2017.

30. Woo EY, Chu CS, Goletz TJ, Schlienger K, Yeh H, Coukos G, Rubin SC, Kaiser LR and June CH: Regulatory CD4(+)CD25(+) T cells in tumors from patients with early-stage non-small cell lung cancer and late-stage ovarian cancer. *Cancer Res* 61: 4766-4772, 2001.
31. Peng J, Hamanishi J, Matsumura N, Abiko K, Murat K, Baba T, Yamaguchi K, Horikawa N, Hosoe Y, Murphy SK, *et al*: Chemotherapy induces programmed cell death-ligand 1 overexpression via the nuclear factor- κ B to foster an immunosuppressive tumor microenvironment in ovarian cancer. *Cancer Res* 75: 5034-5045, 2015.
32. Gammaitoni L, Giraudo L, Macagno M, Leuci V, Mesiano G, Rotolo R, Sassi F, Sanlorenzo M, Zaccagna A, Pisacane A, *et al*: Cytokine-induced killer cells kill chemo-surviving melanoma cancer stem cells. *Clin Cancer Res* 23: 2277-2288, 2017.
33. Rong XX, Wei F, Lin XL, Qin YJ, Chen L, Wang HY, Shen HF, Jia LT, Xie RY, Lin TY, *et al*: Recognition and killing of cancer stem-like cell population in hepatocellular carcinoma cells by cytokine-induced killer cells via NKG2d-ligands recognition. *Oncol Immunology* 5: e1086060, 2015.
34. Long EO: ICAM-1: Getting a grip on leukocyte adhesion. *J Immunol* 186: 5021-5023, 2011.
35. Arnold JM, Cummings M, Purdie D and Chenevix-Trench G: Reduced expression of intercellular adhesion molecule-1 in ovarian adenocarcinomas. *Br J Cancer* 85: 1351-1358, 2001.
36. de Groote ML, Kazemier HG, Huisman C, van der Gun BT, Faas MM and Rots MG: Upregulation of endogenous ICAM-1 reduces ovarian cancer cell growth in the absence of immune cells. *Int J Cancer* 134: 280-290, 2014.
37. Barsoum IB, Hamilton TK, Li X, Cotechini T, Miles EA, Siemens DR and Graham CH: Hypoxia induces escape from innate immunity in cancer cells via increased expression of ADAM10: Role of nitric oxide. *Cancer Res* 71: 7433-7441, 2011.
38. Terry S, Buart S, Tan TZ, Gros G, Noman MZ, Lorens JB, Mami-Chouaib F, Thiery JP and Chouaib S: Acquisition of tumor cell phenotypic diversity along the EMT spectrum under hypoxic pressure: Consequences on susceptibility to cell-mediated cytotoxicity. *Oncol Immunology* 6: e1271858, 2017.
39. Wan J, Wu W, Che Y, Kang N and Zhang R: Low dose photodynamic-therapy induce immune escape of tumor cells in a HIF-1 α dependent manner through PI3K/Akt pathway. *Int Immunopharmacol* 28: 44-51, 2015.
40. Lee YH, Bae HC, Noh KH, Song KH, Ye SK, Mao CP, Lee KM, Wu TC and Kim TW: Gain of HIF-1 α under normoxia in cancer mediates immune adaptation through the AKT/ERK and VEGFA axes. *Clin Cancer Res* 21: 1438-1446, 2015.
41. Lu Y, Hu J, Sun W, Duan X and Chen X: Hypoxia-mediated immune evasion of pancreatic carcinoma cells. *Mol Med Rep* 11: 3666-3672, 2015.
42. Wei F, Rong XX, Xie RY, Jia LT, Wang HY, Qin YJ, Chen L, Shen HF, Lin XL, Yang J, *et al*: Cytokine-induced killer cells efficiently kill stem-like cancer cells of nasopharyngeal carcinoma via the NKG2D-ligands recognition. *Oncotarget* 6: 35023-35039, 2015.
43. Sawada T1: Kimura K, Nishihara T, Onoda N, Teraoka H, Yamashita Y, Yamada N, Yashiro M, Ohira M, Hirakawa K. TGF-beta1 down-regulates ICAM-1 expression and enhances liver metastasis of pancreatic cancer. *Adv Med Sci* 51: 60-65, 2006.
44. Bessa X, Elizalde JI, Mitjans F, Piñol V, Miquel R, Panés J, Piulats J, Piqué JM and Castells A: Leukocyte recruitment in colon cancer: Role of cell adhesion molecules, nitric oxide, and transforming growth factor beta1. *Gastroenterology* 122: 1122-1132, 2002.
45. Ohga E and Matsuse T: The relationship between adhesion molecules and hypoxia. *Nihon Rinsho* 58: 1587-1591, 2000 (In Japanese).
46. Thichanpiang P, Harper SJ, Wongprasert K and Bates DO: TNF- α -induced ICAM-1 expression and monocyte adhesion in human RPE cells is mediated in part through autocrine VEGF stimulation. *Mol Vis* 20: 781-789, 2014.
47. Li J, Chen L, Xiong Y, Zheng X, Xie Q, Zhou Q, Shi L, Wu C, Jiang J and Wang H: Knockdown of PD-L1 in human gastric cancer cells inhibits tumor progression and improves the cytotoxic sensitivity to CIK therapy. *Cell Physiol Biochem* 41: 907-920, 2017.
48. Chen CL, Pan QZ, Zhao JJ, Wang Y, Li YQ, Wang QJ, Pan K, Weng DS, Jiang SS, Tang Y, *et al*: PD-L1 expression as a predictive biomarker for cytokine-induced killer cell immunotherapy in patients with hepatocellular carcinoma. *Oncol Immunology* 5: e1176653, 2016.
49. Ren X, Ma W, Lu H, Yuan L, An L, Wang X, Cheng G and Zuo S: Modification of cytokine-induced killer cells with chimeric antigen receptors (CARs) enhances antitumor immunity to epidermal growth factor receptor (EGFR)-positive malignancies. *Cancer Immunol Immunother* 64: 1517-1529, 2015.